

Experimental demonstration of weak-light laser ranging and data communication for LISA

Juan José Esteban,^{1,2,*} Antonio F. García,^{1,2} Simon Barke,^{1,2}
Antonio M. Peinado,³ Felipe Guzmán Cervantes,^{1,2} Iouri Bykov,^{1,2}
Gerhard Heinzl,^{1,2} and Karsten Danzmann^{1,2}

¹Max-Planck Institute for Gravitational Physics (Albert-Einstein Institute),
Callinstrasse 38, 30167 Hannover, Germany

²QUEST Center for Quantum Engineering and Space-Time Research,
Leibniz University of Hannover, Germany

³Department of Signal Theory, Networking and Communications,
University of Granada, Faculty of Science - C.P. 18071, Spain

*juan.jose.esteban@aei.mpg.de

Abstract: Interferometric gravitational wave detectors with an unequal and time-varying arm length configuration like the Laser Interferometer Space Antenna rely on time-delay interferometry (TDI) for laser frequency noise subtraction. However, the TDI algorithm requires a laser ranging scheme with meter accuracy over a five million kilometer arm length. At the end of each arm only about 100 pW of light power will be detected for gravitational wave measurements and only 1% of this power can be used for laser ranging in order to avoid degradation in the phase stability of the science measurements. Here, we present the first experimental demonstration of such a ranging scheme at 1 pW power levels using a Direct Sequence Spread Spectrum (DS/SS) modulation. This type of modulation also enables optical communication by encoding data with ranging signals and provides significant noise reduction against spurious interfering signals for bidirectional ranging. Experimental results show ranging measurements of 42 cm at 3 Hz and the viability of highly reliable data transfer at several kilobits per second.

© 2011 Optical Society of America

OCIS codes: (120.3180) Interferometry; (280.3400) Laser range finder; (060.2605) Free-space optical communication.

References and links

1. T. E. Bell, "Gravitational astronomy: hearing the heavens," *Nat. News* **452**, 18–21 (2008).
2. LISA International Science Team (LIST), "LISA assessment study report: yellow book," *Eur. Space Agency*, 1–141 (2011).
3. NASA Goddard Space Flight Center, "Laser interferometer space antenna: sciencecraft description," LISA-SC-DD-0001, 1–106, (2009).
4. LISA Frequency Control Study Team, ESA Report No. LISA-JPL-TN-823, (2009).
5. D. A. Shaddock, B. Ware, R.E. Spero, and M. Vallisneri, "Postprocessed time-delay interferometry for LISA," *Phys. Rev. D* **70**(8), 1101–1106 (2004).
6. G. de Vine, B. Ware, K. McKenzie, R. E. Spero, W. M. Klipstein, and D. A. Shaddock, "Experimental demonstration of time-delay interferometry for the laser interferometer space antenna," *Phys. Rev. Lett.* **104**(21), 11031–11034 (2010).

7. R. Ziemer and R. Peterson, *Digital Communications and Spread Spectrum Systems* (Macmillan, 1985).
8. G. Heinzel, "Ranging with pseudo-random noise," LISA International Science Team (LIST) meeting, (2002).
9. G. Heinzel, J. J. Esteban, S. Barke, M. Otto, Y. Wang, A. F. Garcia, and K. Danzmann, "Auxiliary functions of the LISA laser link: ranging, clock noise transfer and data communication," *Class. Quantum Grav.* **28**(9), 4008–4019 (2011).
10. J. J. Esteban, A. F. Garcia, J. Eichholz, A. M. Peinado, I. Bykov, G. Heinzel, and K. Danzmann, "Ranging and phase measurements for LISA," *J. Phys.: Conf. Ser.* **228**(1), 2045–2053 (2010).
11. A. Sutton, K. McKenzie, B. Ware, and D. A. Shaddock, "Laser ranging and communications for LISA," *Opt. Express* **18**(20), 20759–20773 (2010).
12. G. Heinzel, C. Braxmaier, K. Danzmann, P. Gath, J. Hough, O. Jennrich, U. Johann, A. Rüdiger, M. Sallusti, and H. Schulte, "LISA interferometry: recent developments," *Class. Quantum Grav.* **23**(8), 119–124 (2006).
13. O. Jennrich, "LISA technology and instrumentation," *Class. Quantum Grav.* **26**(15), 3001–3033 (2009).
14. P. W. McNamara, "Weak-light phase locking for LISA," *Class. Quantum Grav.* **22**(10), 243–247 (2005).
15. B. Parkinson and J. J. Spilker, "Global positioning system : theory and applications," *Am. Inst. Astronaut. Aeronaut.* (1996).
16. E. Morrison, B. J. Meers, D. I. Robertson, and H. Ward, "Experimental demonstration of an automatic alignment system for optical interferometers and automatic alignment of optical interferometers," *Appl. Opt.* **33**(22), 5037–5040 (1994).
17. E. Morrison, B. J. Meers, D. I. Robertson, and H. Ward, "Automatic alignment of optical interferometers," *Appl. Opt.* **33**(22), 5041–5049 (1994).
18. G. Hechenblaikner, R. Gerndt, U. Johann, P. Luetzow-Wentzky, V. Wand, H. Audley, K. Danzmann, A. F. Garcia, G. Heinzel, M. Nofrarias, and F. Steier, "Coupling characterization and noise studies of the optical metrology system onboard the LISA Pathfinder mission," *Appl. Opt.* **49**(29), 5665–5677 (2010).
19. M. Armano, M. Benedetti, J. Bogenstahl, D. Bortoluzzi, P. Bosetti, N. Brandt, A. Cavalleri, G. Ciani, I. Cristofolini, A. M. Cruise, K. Danzmann, I. Diepholz, G. Dixon, R. Dolesi, J. Fauste, L. Ferraioli, D. Fertin, W. Fichter, M. Freschi, A. Garca, C. Garca, A. Grynagier, F. Guzman, E. Fitzsimons, G. Heinzel, M. Hewitson, D. Hollington, J. Hough, M. Hueller, D. Hoyland, O. Jennrich, B. Johlander, C. Killow, A. Lobo, D. Mance, I. Mateos, P. W. McNamara, A. Monsky, D. Nicolini, D. Nicolodi, M. Nofrarias, M. Perreux-Lloyd, E. Plagnol, G. D. Racca, J. Ramos-Castro, D. Robertson, J. Sanjuan, M. O. Schulte, D. N. A. Shaul, M. Smit, L. Stagnaro, F. Steier, T. J. Sumner, N. Tateo, D. Tombolato, G. Vischer, S. Vitale, G. Wanner, H. Ward, S. Waschke, V. Wand, P. Wass, W. J. Weber, T. Ziegler, and P. Zweifel, "LISA pathfinder: the experiment and the route to LISA," *Class. Quantum Grav.* **26**(9), 4001–4019 (2009).

1. Introduction

The Laser Interferometer Space Antenna (LISA) is a space mission designed to observe a broad range of astrophysical and cosmological sources of gravitational waves in the low-frequency (mHz) band [1–3]. LISA consists of a three spacecraft constellation orbiting around the Sun at 50×10^6 km behind the Earth in a near-equilateral triangle formation with a side length of 5×10^6 km. Three bidirectional laser links will be established between satellites, enabling the formation to act as a huge distributed interferometer for monitoring the relative changes in the optical path length induced by gravitational waves. To achieve its strain sensitivity goal of 10^{-22} , the inter-satellite laser links will be continuously monitored with picometer accuracy through precise measurements of the optical carrier phases with an allocated noise budget of 1×10^{-6} cycles/ $\sqrt{\text{Hz}}$.

As a consequence of the orbital motion, the length of the three interferometric arms will be unequal and time-varying with a maximum mismatch of $\Delta L \approx 5 \times 10^4$ km. This unequal arm length configuration combined with a typical free-running laser frequency noise of $\approx 1 \times 10^4 f^{-1}$ Hz/ $\sqrt{\text{Hz}}$ would result in a phase noise of $\approx 1 \times 10^8$ cycles/ $\sqrt{\text{Hz}}$, exceeding the required performance for LISA by many orders of magnitude. Two complementary techniques will be implemented to achieve the required phase sensitivity [4]. Initially, a laser pre-stabilization will reduce the free-running frequency noise to hundreds of Hz/ $\sqrt{\text{Hz}}$ in the millihertz band. A second technique, called Time Delay Interferometry (TDI) [5], will employ precise measurements of the absolute inter-satellite distance in order to synthesize an equal arm length interferometer by post-processing on ground. This technique is limited by residual laser frequency noise and relies in the knowledge of the absolute arm length mismatch with 1 meter

resolution [4, 6]. However, a ranging accuracy of meters is beyond the performance of the most advanced positioning techniques on ground for deep space missions, and therefore, precise measurements on board each spacecraft will be conducted as ancillary functions of the laser links.

An on board laser ranging system based on an optical Direct Sequence Spread Spectrum (DS/SS) modulation is a viable technology to be incorporated into the precise inter-satellite interferometry system. Through such an integration, the metrology system will provide both relative measurements at picometer accuracy and absolute ranging measurements at sub-meter accuracy. Two additional benefits can be simultaneously accomplished by applying this modulation scheme. Firstly, it enables inter-satellite communication by encoding data in the ranging signals [7]. Secondly, it can be implemented using only a small fraction of the available laser power so that it can be integrated in the optical metrology system without interferometric performance degradation.

The use of DS/SS modulation applied to space-based gravitational wave detectors was initially suggested in 2002 [8], and recently the feasibility of this technique has been verified [9–11]. In this paper, we report the first experimental results of such a scheme considering the effect of the inter-spacecraft motion and the low light power available (1 pW) for ranging in LISA. Section 2 gives an overview of the optical metrology system based on a simplified scheme of a single LISA arm. Section 3 describes the architecture of our prototype for ranging and data communication as well as its impact on the fidelity of the phase measurements. Finally, in Section 4 we report on the implementation of the proposed ranging scheme in an optical test-bed and the results obtained in weak light conditions.

2. Optical Metrology System Overview

A simplified schematic of the optical metrology system for one LISA arm is represented in Fig. 1. Two satellites separated by five million kilometer shield two free floating test masses from external disturbances. The test masses serve as reference points of an inter-satellite interferometry system. Local interferometers monitor position and orientation of each test mass to their respective optical benches [12, 13]. To monitor relative displacement between optical benches, laser beams with a transmitted light power of 1 W are exchanged between satellites. Due to diffraction losses of the beam over the long distance propagation and additional optical losses on the bench, only around 100 pW are detected at the remote spacecraft [14]. The weak beam received is directly brought to interference with a local laser on the optical bench, thus providing a beat note at their frequency difference. The phase of the resulting beat note is then measured with respect to its on board clock in a phase measurement system (PMS), and used as control signal to return the local laser as a high power phase replica of the incoming beam. In LISA, the Doppler shifts produced by orbital motion of the spacecraft (relative velocity up to ± 20 m/s) lead to a design of the beat note in the range between 2 to 20 MHz. To achieve the required phase sensitivity, $\tilde{\phi} \simeq 1 \times 10^{-6}$ cycle/ $\sqrt{\text{Hz}}$ for a beat note up to 20 MHz, the necessary clock timing jitter would be approximately $\delta t \leq \tilde{\phi}/20 \text{ MHz} \simeq 50 \text{ fs}/\sqrt{\text{Hz}}$. This timing stability is beyond the performance of the most stable clocks available in space-based applications. Consequently the optical metrology system requires a clock noise removal scheme to subtract the excess phase noise that couples into the science measurements. To this end, each spacecraft clock is up-converted to GHz frequencies and phase modulated onto the laser links using 10% of the light power. In this way, the clock jitter is intentionally amplified in the resulting sideband-to-sideband beat note so that its phase noise performance can be relaxed, i.e., for clock sidebands of 2 GHz, the phase readout requirement can be relaxed by a factor of $2 \text{ GHz}/20 \text{ MHz} = 100$. Finally, the phase measurements of the sideband beat notes on each satellite are transmitted to ground for TDI post-processing and for clock noise removal [6].

Furthermore, the phasemeter provides the input signal for ranging and data communication. To this end, a pseudo-random noise (PRN) sequence encoded with data is phase modulated onto each laser using 1% of the light power before being transmitted to the remote spacecraft. The PRN modulation is recovered as phase transitions at the remote phasemeter output when both control loops, the offset laser phase-locking and the phasemeter, are locked. A delay-locked loop (DLL) architecture is implemented for PRN tracking and delay measurements. It aligns the local PRN reference to the incoming code via correlation of both sequences, while the data information is directly decoded from the PRN sequences.

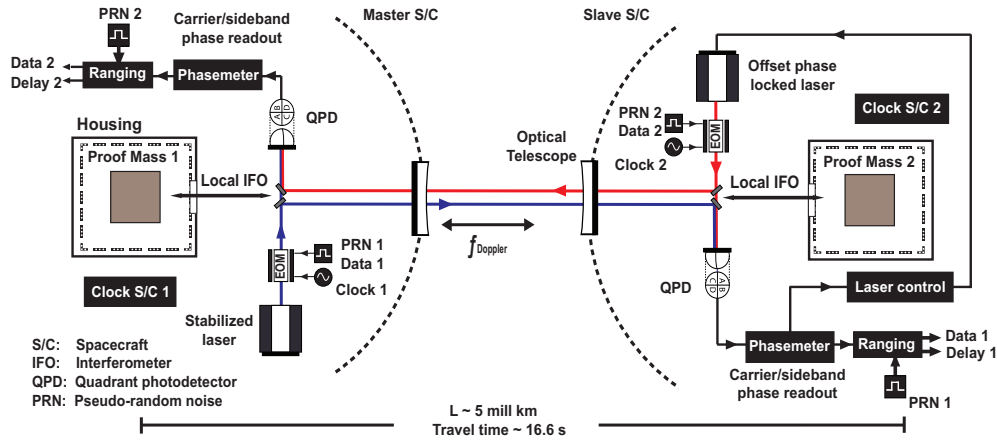


Fig. 1. Simplified diagram of the optical metrology system for an interferometric arm in LISA. The metrology system with data communication capability provides measurements of the relative path length displacements between two free-floating test masses, inter-satellite clock jitter and the absolute arm length distance. On each satellite, the on board clock and pseudo-random noise (PRN) sequences encoded with data information are phase modulated onto a laser using an electro-optic modulator (EOM). Both lasers, labeled as master and slave, are exchanged between satellites and offset phase locked to generate the heterodyne beat signals. Each satellite measures the phase of their resulting beat signals in the phase measurement system (PMS), which is also employed for PRN demodulation to perform ranging and data transfer.

3. Ranging and Data Transfer

The ranging scheme is identical for each of the six lasers in LISA and it provides six independent delay measurements referenced to the three unsynchronized clocks. Therefore, a negligible cross-correlation between codes is desirable to reduce the interference noise from codes modulated onto different lasers. Thus, an important design aspect in the ranging performance is the orthogonality property of the pseudo-codes. The codes show an autocorrelation peak at zero delay and vanishing autocorrelation for other delays. This peak serves as a delay detector and as a time-stamp if the start of the PRN is synchronized with the clock of the remote spacecraft. Binary data are encoded with the PRN sequence at lower rates by bitwise operation (XOR) of both sequences so the code length is divided into several data periods. For each data period the sign of the code autocorrelation is retained, being inverted for a different data bit. Adding the absolute value of each data period over a full code-length, the correlation function is recovered for code acquisition and tracking. By applying this method for data encoding, the ranging signal in-

creates its data rate capability without a significant reduction in the code tracking performance of the system, as shown in the results of Section 4. The design parameters of the pseudo-codes are described in Fig. 2. In contrast to standard families of encoding sequences, e.g., Gold codes employed in satellite navigation [15], the designed set of pseudo-codes was obtained by numerical optimization to enhance their correlation properties and with an even length of 1024 chips to simplify their subdivision into data bits. The codes are sampled at 50 MHz, run at a chipping rate of 1.5 Mbps (50 MHz/32 samples) limited by the lower frequency of the beat note, and encoded with data streams at a maximum data rate of 24.4 kbps (50 MHz/2048 samples). The data-encoded PRN signal provides a delay resolution of $20\text{ ns} \simeq 6\text{ m}$ with an update rate of 1.5 kHz (50 MHz/32768 samples). Since the on board computer in LISA requires regular update rates between 3-10 Hz, the delay measurements are averaged down to achieve sub-meter absolute distance resolution (see Section 4). Note that under these design parameters, the codes are periodic every 200 km over the 5 million kilometers, and therefore an initial positioning system is required. The deep-space network (DNS) yields an absolute inter-satellite distance with a resolution of $\approx 25\text{ km}$, and thus after this initial positioning, a more accurate distance determination will be achieved using the proposed DLL architecture.

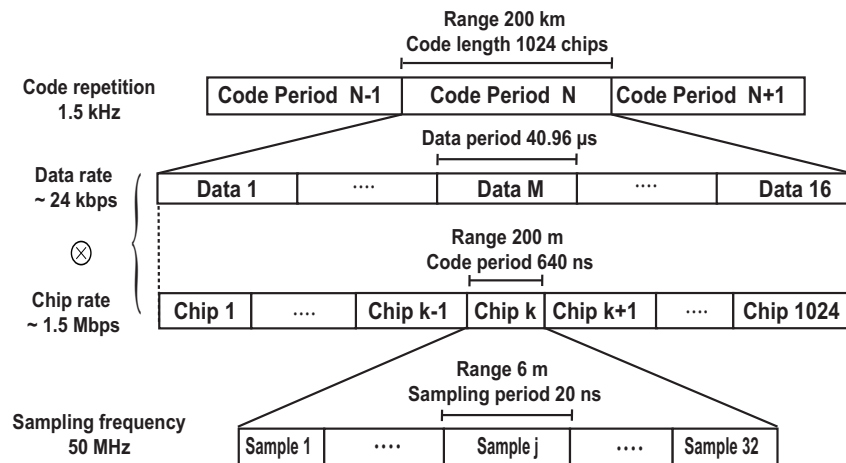


Fig. 2. Design parameters of the ranging system. Code length of 1024 chips running at 1.5 Mbps encoded with a data rate at 24.4 kbps and sampled at 50 MHz. The design parameters enable a ranging system with a range ambiguity of 200 km, a distance resolution of 6 m, and a measurement rate of 1.5 kHz.

3.1. Low-depth PRN Phase Modulation

As described in Fig. 3, both phasemeter and ranging architectures were integrated in a Field-Programmable Gate Array (FPGA) processor. The core of the phasemeter implements a digital phase-locked loop (DPLL) architecture to lock the phase of a Numerically Controlled Oscillator (NCO) to the incoming beat note. A phase and amplitude detector based on an in-phase/quadrature (I/Q) demodulator is used to control the NCO in a feedback loop. The phase measurement is built in a floating-point unit as the sum of raw phase estimations from the NCO and the arctangent of the I and Q components, while the amplitude of the beat note is obtained as $\sqrt{I^2 + Q^2}$. For a single phasemeter channel, the optical metrology system performs precise longitudinal displacement measurements, which gives the proposed phasemeter architecture advanced capabilities. It can provide angular measurements for precise laser pointing or

satellite drag-free control using quadrant photo detectors by subtracting phase measurements from different quadrants [16, 18], as it is being implemented on the precursor mission LISA Pathfinder [19].

For ranging and data communication, the sum of the power in all quadrants gives the entire detected signal power. Once the phase of the beat note has been processed, the PRN code modulated onto the optical carrier appears as phase errors at the Q output, providing the input signal to the DLL. The correlation of the incoming signal is computed with three versions of the same reference PRN: a punctual, an early and a late one. The punctual version is not delayed with respect to the received PRN. The early and late versions of the reference code are spaced with a delay difference lower than one chip period. The punctual correlator is mainly responsible for data recovery and code acquisition, whereas the difference between early and late correlators is used as the error signal in a control loop to update the delay of the code generator to the input signal, thus providing tracking capabilities between the incoming and the local PRN sequences.

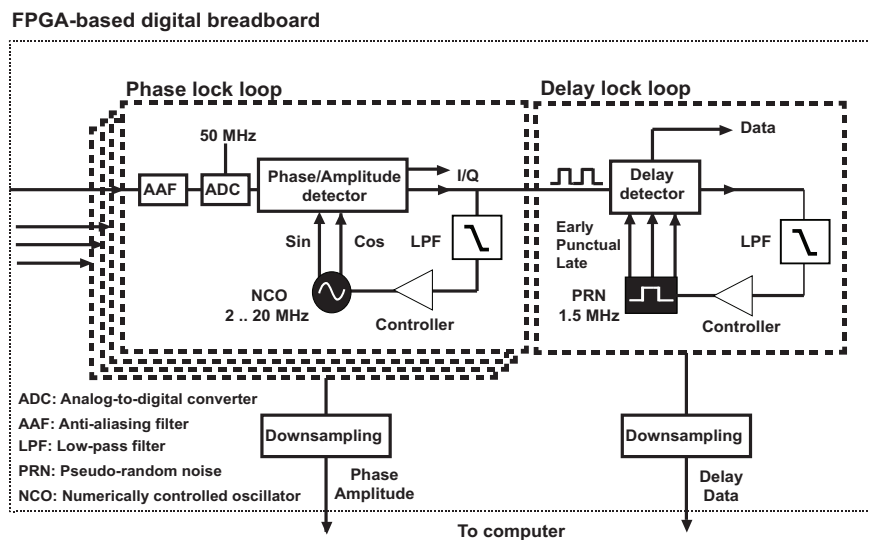


Fig. 3. General architecture of the digital control loops implemented for phase measurements, ranging and data transfer.

PRN modulation spreads the carrier power over a large frequency range, causing fast phase transitions with an amplitude variation proportional to the modulation depth. In contrast to standard ranging methods, the proposed system uses a low-depth PRN modulation scheme in order to reduce both optical power allocated to the PRN modulation and residual carrier phase noise due to fast PRN transitions.

In order to assess the impact of the ranging system in the phase stability of the main science measurements, the phasemeter performance was tested at different PRN modulation depths. To this end, a FPGA-based signal generator was used to produce a LISA-like signal structure with two data-encoded PRN sequences, providing the input signal for the phasemeter and the ranging system. The electrical spectrum of the phasemeter input signals and the noise spectral density of the resultant measurements are shown in Fig. 4. The phasemeter measurements were subtracted from a nominal phase at a constant heterodyne frequency, such that the differential phase noise was due to PRN modulation.

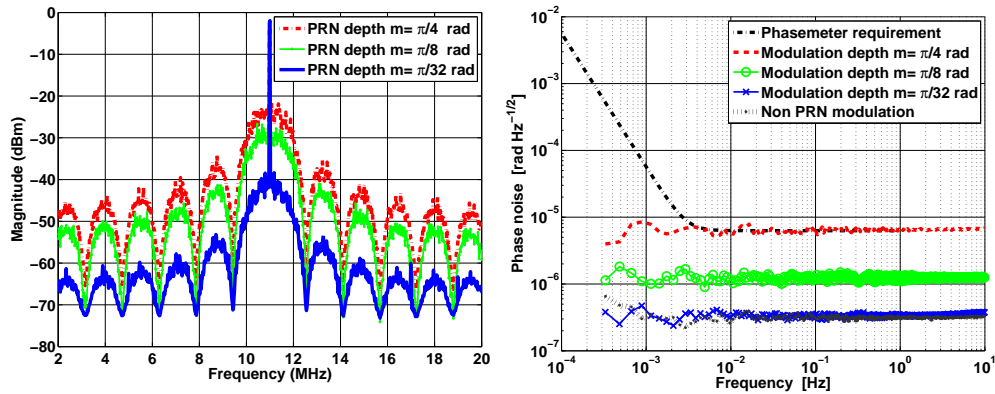


Fig. 4. (Left side) Electrical spectrum of the phasemeter input signal at different modulation depths. (Right side) Noise power spectral density comparing the impact of different PRN modulation depths in the phasemeter performance. The measurements modulate two PRN sequences (local and remote pseudo-codes) encoded with data streams at 24.4 kbps.

For the designed DPLL architecture with a bandwidth of about 100 kHz, the residual phase noise produced by PRN modulation was successfully suppressed. The overall phasemeter performance achieved picometer accuracy even in presence of high modulation depths, i.e., $\pi/4 \simeq 0.78$ rad. By applying modulation depths at $\pi/32 \simeq 0.1$ rad, which corresponds to an equivalent light power below 1%, the PRN modulation produced a broadband phase noise about one order of magnitude below the required phase fidelity for LISA.

4. Optical Testing for Laser Ranging and Data Transfer

The low-light power available for ranging and data communication (1 pW) yields a ranging signal below the shot noise level. In such conditions, the shot noise introduced by the lasers at the photodetector limits the ranging accuracy and increases the data errors for optical communication. A heterodyne interferometer was built to demonstrate the sub-meter ranging accuracy and data communication at several kilobits per second in a weak-light environment, taking into account realistic LISA-like conditions, such as time-variation of ranging signals due to satellite motion and clock sideband interferences. Figure 5 shows a schematic diagram of the experimental setup. Two Nd:YAG lasers were used as continuous light sources at 1064 nm. Both lasers were linearly polarized and isolated from optical feedback before being coupled into a fiber. For each laser, a fiber-coupled electro-optic modulator (EOM) was used to provide the optical phase modulation of data-encoded PRN signals and clock sidebands at 2 GHz using 1% and 10% of the light power respectively. The PRN modulation onto the local laser was then included, through a phase modulation of a different pseudo-noise sequence, to provide the spurious interfering code that is a side-effect of the bidirectional ranging scheme. To reduce the detected light to ~ 100 pW on the photodiode, a series of grey filters were used to drastically decrease the power level of the master laser before interfering at the optical bench. Using slow (thermal) and fast (piezoelectric) frequency actuators, a weak-light laser offset phase locking method generated the heterodyne beat signal between the two lasers. An InGaAs photodetector with transimpedance amplifier sensed the beat note, which was digitized and processed in a custom-designed breadboard with a space-compatible FPGA unit.

Figure 6 shows a comparison of the optical beat note spectrum measured in the laboratory for normal light ($P_M = 10$ nW) and weak-light environments, respectively. In normal-light con-

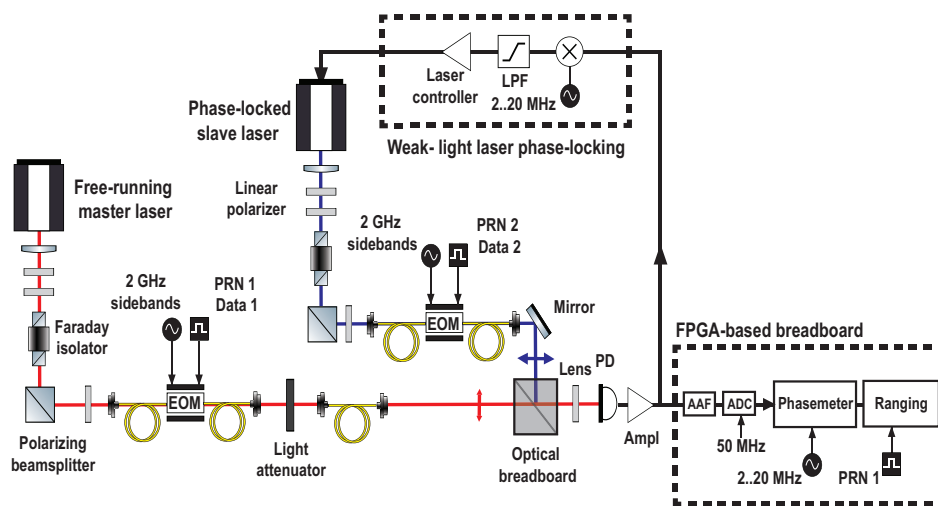


Fig. 5. Simplified schematic of the experimental setup used to test the laser modulation scheme.

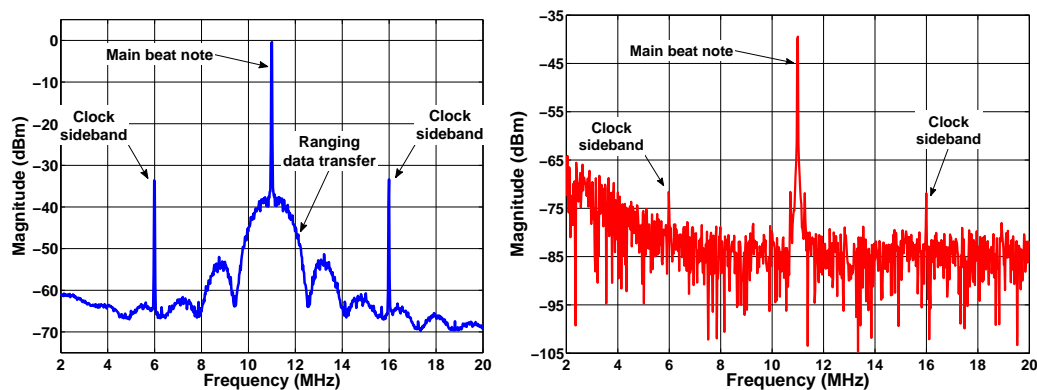


Fig. 6. Spectrum comparison of the beat note for normal-light (left side) and weak-light (right side) environments.

ditions the PRN modulation appears as sidelobes in the main carrier. An attenuation in the beat note power of 40 dB is observable for the weak-light environment, resulting in a noise floor above the ranging signals. Figure 7 shows the corresponding rms ranging accuracy in meters. The tracked signal is a time-varying PRN code with an equivalent velocity of ± 20 m/s. The ranging signal modulated onto the local laser is also time-varying such that it performs a cross-correlation distribution for all possible delays. Under these conditions, experimental results demonstrate a ranging rms noise of 42 cm at 3 Hz for data rates of 24.4 kbps at 1 pW power levels. The raw data transmitted has a bit error rate (BER) of up to 26×10^{-3} . For data error corrections, a FPGA-based Reed-Solomon (RS) encoding technique is applied to demonstrate the viability of reliable optical communications. To this end, a RS(n=15,k=9) scheme with m = 4-bit symbols has been implemented, where n corresponds to the code length and k refers to the data symbols per code. This includes (n-k) parity symbols, resulting in an effective data rate of 14.6 kbps, and subsequently an equivalent receiver sensitivity of ≈ 366 photons/bit with coding for the standard 10^{-9} BER in coherent communication systems.

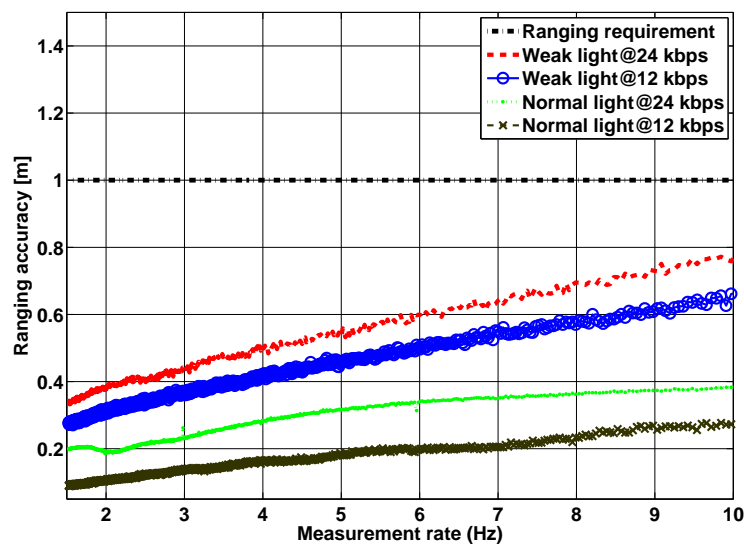


Fig. 7. Ranging rms noise of the optical ranging measurements for different data rates and in the presence of LISA-like noise sources, including interference with a second PRN and simulated inter-spacecraft velocity.

Table 1. Ranging Accuracies for Different Data Rates and Different Optical Power Conditions

Code parameters		Ranging rms noise		Bit Error Rate (BER)	
Optical Power	Data rate	10 Hz	3 Hz	Raw data	Reed-Solomon
10 nW	12 kbps	25 cm	15 cm	No error detected	No required
10 nW	24 kbps	38 cm	22 cm	No error detected	No required
1 pW	12 kbps	62 cm	38 cm	$< 6 \times 10^{-4}$	No error detected
1 pW	24 kbps	76 cm	42 cm	$< 26 \times 10^{-3}$	No error detected

As shown in Table 1, this technique provides the necessary data correction to achieve an error-free optical transmission. The fundamental limit of the measurement under weak-light conditions is shot noise. An estimate of the rms ranging error in meters due to shot noise can be computed as $\sigma \approx c \cdot T_c / \sqrt{SNR_L}$ [15], where c is the speed of light, SNR_L is the signal-to-noise ratio in the loop bandwidth B_w (3-10 Hz), and T_c is the chip period (1/1.5 MHz). For a received carrier-power-to-noise density ratio (C/N_0) of ≈ 64 dB-Hz ($SNR_L = C/N_0 B_w$) at the input of the ranging system, i.e., by applying a modulation depth of 0.1 rad, and a total incoming phase noise contribution due to the shot noise of $\approx 58 \mu\text{rad}/\sqrt{\text{Hz}}$, we obtain a theoretical accuracy limit of ≈ 20 cm at 3 Hz. Our measured results are a factor of two above this level. A more detailed noise investigation, requiring additional testing is necessary to identify the origin of the excess ranging noise and to quantify the noise contribution of effects like data transfer and interference of the second PRN signal.

5. Conclusion

We have demonstrated operation of a ranging scheme at sub-meter accuracy with data communication capabilities based on a laser transponder configuration with heterodyne detection at picowatt power levels. Such a system can be integrated with precise laser interferometry at picometer accuracy and offers a promising technology for future optical satellites given the advanced laser link functionalities. In particular, it enables clock comparison of remote stations, Doppler estimations through optical phase tracking, and wavefront tilt measurements for precise laser pointing techniques or satellite drag-free control.

Acknowledgments

We gratefully acknowledge support by Deutsches Zentrum für Luft-und Raumfahrt (DLR) (reference 50 OQ 0501 and 50 OQ 0601) and thank the Deutsche Forschungsgemeinschaft (DFG) for funding the Cluster of Excellence QUEST – Centre for Quantum Engineering and Space-Time Research.